Available online at www.sciencedirect.com
ScienceDirect
Journal of Environmental Sciences 19(2007) 955–960
JOURNAL OF ENVIRONMENTAL SCIENCES
ISSN 1001-0742
CN 11-2629/X
www.jesc.ac.cn

Spatial distribution of aerosol pollution based on MODIS data over Beijing, China

LI Ling-jun[1,*], WANG Ying[2], ZHANG Qiang[3], YU Tong[1], ZHAO Yue[1], JIN Jun[2]

1. Beijing Municipal Environmental Monitoring Center, Beijing 100044, China. E-mail: lilingjun@bjmemc.com.cn
2. Central University for Nationalities, Beijing 100081, China
3. Nanjing Institute of Geography and Limnology, Chinese Academy of Sciences, Nanjing 210008, China

Received 30 August 2006; revised 27 October 2006; accepted 29 November 2006

Abstract

With the help of regression analysis, the relationships were detected between aerosol's contribution to apparent reflectance (ACR) derived from Moderate Resolution Imaging Spectroradiometer (MODIS) on board Terra and hourly PM_{10} mass concentration measured at 30 ground-based locations in Beijing for the August of 2003 and 2004. It was shown that there was a good correlation between the ACR and PM_{10} (linear correlation coefficient, R=0.56). On the basis of this relationship, spatial distribution and possible sources of PM_{10} derived from MODIS were analyzed and two frequently heavily-polluted regions were found, namely downtown of the city and the district near Xishan Mountain. These two regions coincidently are also urban heat island centers. The foundings of this paper will be greatly useful for environmental monitoring and urban planning for Beijing, especially for the 2008 Olympic game to be held in Beijing.

Key words: MODIS; PM_{10}; spatial distribution

Introduction

Atmospheric aerosol plays an important part in radiation balance, and acts as one of the factors resulting in uncertainty in climatic modeling (Charlson *et al*., 1992; Taylorand Penner, 1994; IPCC, 2001). With the global industrialization and urbanization, especially in those metropolis regions, aerosol pollution exerts increasing negative influences on human health and on environment (Berico *et al*., 1997; Beeson *et al*., 1998). Therefore, more and more attention was attached to the aerosol research. However, the present fixed-position observation can no longer meet the requirement in dynamic observation of global atmospheric pollution and environmental changes. The available remote sensing plays an increasingly important role in dynamic observation of local and global eco-environmental changes (Griggs, 1975; Mekler *et al*., 1977; Kaufman and Sendra, 1988; Kaufman *et al*., 2001).

Earth Observing System (EOS) of National Aeronautics and Space Administration (NASA), USA, launched two environmental remote sensing satellites, namely Terra and Aqua. Moderate Resolution Imaging Spectroradiometer (MODIS) is on board these two satellites. The information of aerosol can be extracted from band 1, 3, 7 and 20 of MODIS data. After a large amount of on-the-spot observations with airplanes, Kaufman (1997) and Chu *et al*. (2002) found a good correlation between the reflectance of the near infrared band of 2.13 μm and the surface reflectance of the band of 0.47 μm and 0.66 μm in areas with vegetated surface, so that they successfully studied aerosol with MODIS data based on this empirical relationship. Following them, some scholars further applied both MODIS data and ground-observation results on aerosol research (Chu *et al*., 2003; Hutchison, 2003; Wang and Christopher, 2003).

Particulate matter is the dominant atmospheric pollutant for Beijing. The State Environmental Protection Administration of China has issued atmospheric quality standards, which evaluated air quality by air pollution index (API) based on the influences of air pollutions on human health. To be safe to human health, the concentration of PM_{10} should be lower than 150 $\mu g/m^3$.

There are more than 30 ground-based observatory stations in Beijing. Although the measurement precision is good enough, the dispersed stations cannot cater for the demand for spatial distribution and transportation analysis of atmosphere pollutants. Meanwhile, MODIS data are suitable for regional analysis of spatial distribution and dynamic analysis of spatial transportation of atmosphere pollutants. In recent years, the application of MODIS data is being received more and more concerns from academic circle (Kaufman *et al*., 1997; Mao *et al*., 2002; Chu *et al*., 2002), which focus mainly on inversion optical

Project supported by the "985 Project" by the State Ministry of Education, China (No: CUN985-3-3). *Corresponding author.
E-mail: lilingjun@bjmemc.com.cn.

thickness. This study discusses its application to ground air pollution that is in close relation to human health and will attract more attention from the world, because of the 29th Olympic game in Beijing 2008. This article aims to analyze the spatial distribution of ground-surface PM_{10} in Beijing based on MODIS data together with ground-based observations, then further analyzed the pollution characteristics and possible sources. Although the products of MODIS were mainly applied for monitoring $PM_{2.5}$ (Hutchison, 2003; Wang and Christopher, 2003), PM_{10} data were employed for the lack of routine $PM_{2.5}$ monitoring in Beijing, and for there is good correlation between $PM_{2.5}$ and PM_{10} (Yu *et al*., 2004).

1 Materials and methods

The analysis steps of this study are as follows: (1) to decide reflectance and radiance of related bands of MODIS; (2) to eliminate pixels with noise from clouds based on infrared threshold method and to eliminate pixels with higher brightness; (3) to analyze the role of aerosol on reflectance, assuming that the absorption and dispersion of atmospheric molecules in Beijing area are constant under the condition that the air state is stable (it is named as aerosol's contribution to apparent reflectance (ACR) here); (4) ACR demonstrates the pollution degree of atmospheric aerosols, which is in good correlation with concentration of the particulate pollutant on the ground surface. This correlation will be used to decide the horizontal distribution of particulate pollution on the surface.

1.1 Reflectance and radiance

MODIS level 1B data include top of the atmosphere (TOA) radiance and reflectance, which are corrected and fully calibrated in physical units at the instrument's spatial and temporal resolutions. Both the TOA radiance and reflectance are stored in a Scientific Data Set Object, Scaled integer (SI). The scaled integer is a 16-bit unsigned integer which can be converted into radiance or reflectance with the following equations:

$$\rho^*_{\cos(\theta)} = S_{\text{ref}} \times (\text{SI} - INT_{\text{ref}}) \quad (1)$$

$$L_{\cos(\theta)} = S_{\text{rad}} \times (\text{SI} - INT_{\text{rad}}) \quad (2)$$

Where, ρ^* is the apparent reflectance (ref); L is the apparent radiance (rad); θ is the zenith angle, SI is the scaled integer, S_{ref} and S_{rad} are scale factor, INT_{ref} and INT_{rad} are offsets.

1.2 Cloud mask and dark pixels

The cloud-free pixels are needed because of strong cloud-radiative forcing. Cloud mask is crucial to distinguish clear from cloudy pixels. Because the brightness temperature of cloud is always much lower than the surrounding non-cloud area, with it cloud pixels can be separated. Cloud-free pixels are selected by using MODIS cloud mask (Ackerman *et al*., 1998).

The radiative effect of aerosol includes backscattering and absorption of direct sunlight and reflection from the surface. For dark surfaces, the scattering effect is dominant while for brighter surfaces the effect is mixed. Therefore, aerosol radiative effect is the strongest for low surface reflectance. It is reported that surface reflectance less than 0.06 is most qualified for the dark targets method, the range of 0.04 to 0.115 was used in this study (Li *et al*., 2003).

1.3 Assessment of PM concentration near the ground

The mass concentration of PM_{10} was measured using the tapered-element oscillating microbalance (TEOM) instrument, which is in the list of standard methods recommended by US Environmental Protection Agency (USEPA, 1990). A Teflon filter was used in this instrument and the sampling flow rate was set to 16.7 L/min. Constant temperature (normally 50°C) was maintained for the air entrance and sampling system to avoid the influence of humidity. Hourly PM_{10} data could be obtained.

Thirty monitoring stations are chosen in this study (Fig.1), including 8 national-level stations and 22 municipal-level stations. These monitoring stations covered districts and counties, involving all countryside, outskirts, industrial areas, major routes of transportation and inhabitancy areas. The exact location of all the sites is decided by GPS.

1.4 Assessment of PM_{10} on the ground

Research on reflectance of ground indicates that there exist linear relations between apparent reflectance of vegetated land at 2.1 μm-band and surface reflectance at bands of 0.66 μm (red light) and 0.47 μm (blue light), respectively. For regions heavily vegetated, 2.1 μm-band ACR is rarely influenced by aerosol particles. Therefore, we can use empirical relationship to estimate surface reflectance at 0.47 μm and 0.66 μm respectively, based upon the reflectance measured at 2.1 μm ($\rho_{0.66} \approx \rho^*_{2.1}/2$, $\rho_{0.47} \approx \rho^*_{2.1}/4$).

As for the red band or blue band, the ACR can be decided as:

$$\text{ACR}_{\text{B}} = \rho^*_{\text{B}} - \rho_{\text{B}} - m_{\text{B}} \quad (3)$$

Where, ρ^*_{B} is the band B apparent reflectance; ρ_{B} is the surface reflectance of band B; m_{B} is the absorbing and scattering rate of air molecules, which is regarded as a

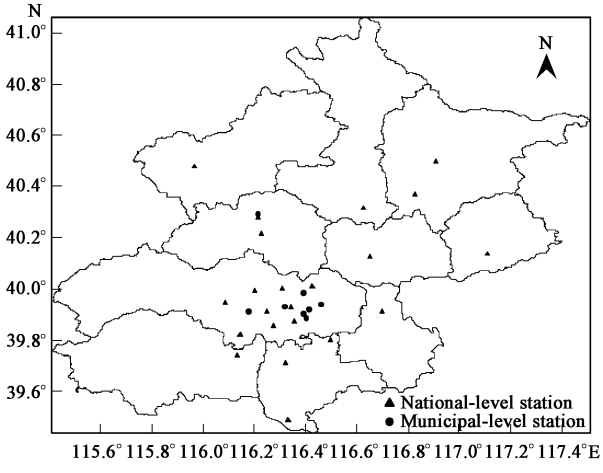

Fig. 1 Thirty observatory sites for PM_{10} in Beijing.

constant in small scale if the air condition is stable. B is the band number; here it means red or blue band. As blue band is influenced greatly by air molecule scattering, we just use red band for analysis in this study. Terra but not Aqua data were chosen here when Aqua passes the zenith, atmospheric mix-layer is more complex, which could bring more error.

In general, PM_{10} concentration descends following an exponential law in vertical direction, but there is a linear correlation between the aerosol integral concentration and air particular matter concentration near ground, also between ACR and the aerosol integral concentration, then the relation between ACR and air particle concentration near the ground can be decided as:

$$\mathrm{ACR} = k \times \mathrm{PM} + b \tag{4}$$

Where, PM is particle concentration, k is the correlation coefficient, which is in close relation with particle types. If ACR=0, it means that there is no aerosol particles in the ideal air, then:

$$\mathrm{ACR_B} = \rho^*_\mathrm{B} - \rho_\mathrm{B} - m_\mathrm{B} = k \times \mathrm{PM} \tag{5}$$

Where, ρ^*_B denotes the apparent reflectance of band B; ρ_B is surface reflectance of band B; PM is hourly PM_{10} data when the satellite passes the zenith, which can be obtained from the ground stations. Only the correlation coefficient k, and air molecules' contribution m_B are unknown values, which can be obtained by statistic relations between known ρ^*_B, ρ_B and PM_{10}, and then concentration of PM_{10} can be obtained by the value of ρ^*_B and ρ_B. m_B depends mainly on the composition and density of air molecules.

2 Results

In August, Beijing is usually covered by luxuriant vegetation, so that more dark pixels and low ground reflectance are available. Furthermore, the Olympic game will be held in August, 2008, MODIS data and the observatory data of PM_{10} from monitoring sites obtained in August of 2003, 2004 will be analyzed in this study to explore the spatial distribution of particles in Beijing. However, August is rainy season in Beijing, so the data of only 14 d out of 62 d during these two years (2003–2004) are qualified. Because of the randomicity of rainy and sunny days, these data are representative and good for present research. There are 387 good ground samples during the 14 d, taking up 92% of all the samples.

Data from MODIS can be explained as $\rho^*_\mathrm{B} - \rho_\mathrm{B} = \mathrm{ACR} + m_\mathrm{B}$. The linear correlation between $\rho^*_\mathrm{B} - \rho_\mathrm{B}$ and PM_{10} is shown in Fig.2. A good linear correlation exists between

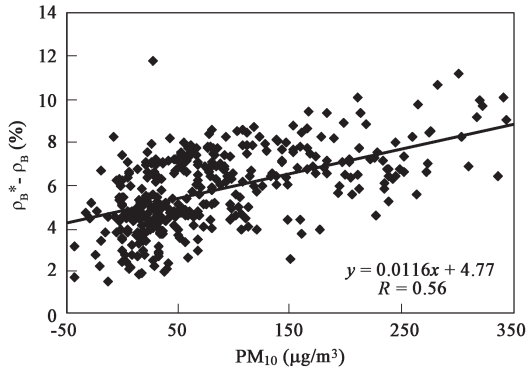

Fig. 2 Relation between ($\rho^*_\mathrm{B} - \rho_\mathrm{B}$) and PM_{10} during August of 2003 and 2004.

ACR and PM_{10} with correlation coefficient of 0.56 (above 95% confidence level). The linear regressive equation is: $\mathrm{ACR} = \rho^*_\mathrm{B} - \rho_\mathrm{B} - m_\mathrm{B} = 0.011 \times PM_{10}$, the constant m_B is 4.77.

In Table 1 it is indicated that relationship between MODIS ACR and hourly PM_{10} concentration was good when the concentration of PM_{10} was higher than 100 μg/m^3, except August 6, 2003, when more clouds exerted negative influence. The correlation coefficient even reached 0.8 on August 4, 2003. However, when the concentration of PM_{10} was lower than 100 μg/m^3, the correlation coefficient was lower than 0.4, and an even minus value.

2.1 Aerosol pollutants in Beijing

It was found that two areas in Beijing were heavily polluted by aerosol pollutant: the downtown of Beijing and piedmont near Xishan Mountain south-west to downtown. These two polluted areas merged when pollution becomes heavy. And sometimes this heavily polluted region even extended to Hebei Province (Fig.3).

Beijing is located in the mid-latitude westerlies, but influenced by Taihang Mountain and Yanshan Mountain at the west and north side respectively, which lead to the occurrence of a stable topographic trough. This topographic trough alters wind flow field, decreases wind speed, and consequently benefits the formation of a pollution convergence zone. This unique geographic location of Beijing results in the mergence of pollutant zones, leading to the origination of mergence highly polluted zone in southwest-northeast direction. Furthermore, Beijing lies in the north side of North China Plain, mountains lying in the west, north and east sides, which makes wind from south or east direction converge at the foot of mountains, then causes the stagnancy of pollutants. The geomorphic features and higher buildings of Beijing prevent the transportation of

Table 1 Relationship between MODIS ACR and hourly PM_{10} mass

	2003/8/4	2003/8/6	2003/8/7	2003/8/11	2003/8/12	2003/8/13	–	–
PM_{10} (μg/m^3)	242	123	35	25	77	226	–	–
Correlation coefficient	0.80	0.34	0.39	0.14	0.08	0.54	–	–
	2004/8/4	2004/8/5	2004/8/17	2004/8/19	2004/8/28	2004/8/29	2004/8/30	2004/8/31
PM_{10} (μg/m^3)	18	137	71	52	10	12	118	25
Correlation coefficient	0.29	0.65	–0.18	0.11	–0.43	0.06	0.51	0.18

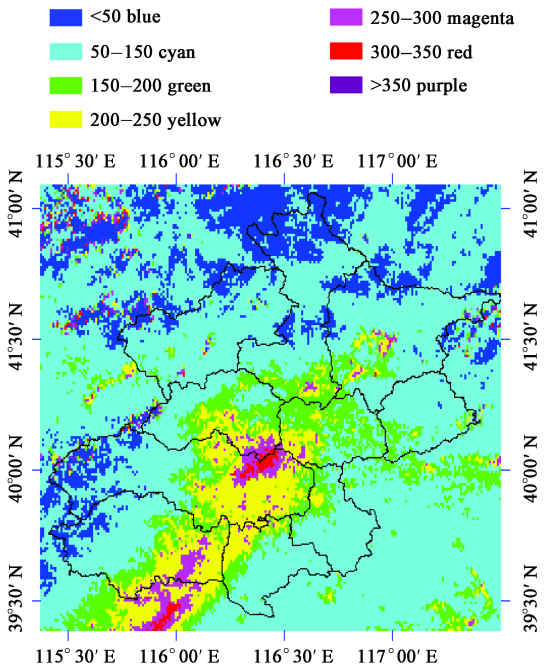

Fig. 3 Distribution of PM_{10} from MODIS in Beijing (2003/8/13; μg/m^3).

pollutants, and lead to heavier pollution in Beijing.

It is inevitable that downtown is one of polluted center. Beijing, as the second largest city in China, is heavily populated and densely loaded with buildings. Large amount of energy is being consumed and considerable wastes are being produced. At the same time, pollution zone expands along main transport lines with a great traffic flow. Air-port Expressway, Badaling Expressway and Jing-Shi Expressway etc., are now pollution stretch zones. Typical air circulation patterns of Beijing also hinder the dispersion of pollution from city to its outskirts, and further intensify the pollution situation of Beijing.

Reasons that piedmont of Xishan Mountain becomes the other polluted center are as follows: (1) it is the direct result of geomorphic features and meteorological situation, and (2) this pollution zone is occupied by many heavy chemical industries and construction industries. The south wind always cannot cross over Xishan Mountain and decelerates before it, forming convergence zone leading to the accumulation of pollutants (Fig.3). When weak north wind enters the plain region through the north-western lower valley or west mountainous regions, a vortex of air flow will be formed, and this leads to the convergence of pollution in Fangshan and Fengtai districts. When stronger wind blows to Beijing, esp. northwest wind, the polluted centers will be weaken and even disappear. The stronger wind transports the pollutants away.

The mentioned-above polluted regions correspond to the center of heat island of Beijing indicated by a former research (Zhang *et al*., 2002). The downtown area locates inside a closed ellipse-shape area with higher temperature, which is the main part of Beijing heat island. The regions along Fengtai, Mentougou and Fangshan are the main zones act as stove, heating the heat island, where the increase of temperature exceeds that in Chaoyang, becoming the sub-center of heat island in Beijing and has been strengthened (Table 2). Urban heat island effect strengthens pollutants accumulation.

2.2 Analysis of PM_{10} on August 4, 2003 in Beijing

Fig.4 shows that the ground PM_{10} concentration is the highest in the border of Tongzhou and Shunyi with two zones with higher concentration of pollutants extending to east and southwest direction, respectively. This MODIS inversed result is in good line with observatory data from ground stations. Relatively lower polluted areas lie between these two higher polluted zones.

On August 4, 2003, air pressure in Beijing became lower gradually; the wind direction was from weak easterly at 08:00 to southern wind at 14:00. South wind led to the converged pollution before Xishan Mountain. South wind also moved the polluted center in the Beijing downtown to the north, forming converged polluted region before the north mountainous areas. Slow wind speed caused obvious accumulation of pollutants and made the two polluted areas join together.

Accumulation of pollutants occurred because of weak air pressure. At 11:00, the average concentration of PM_{10}

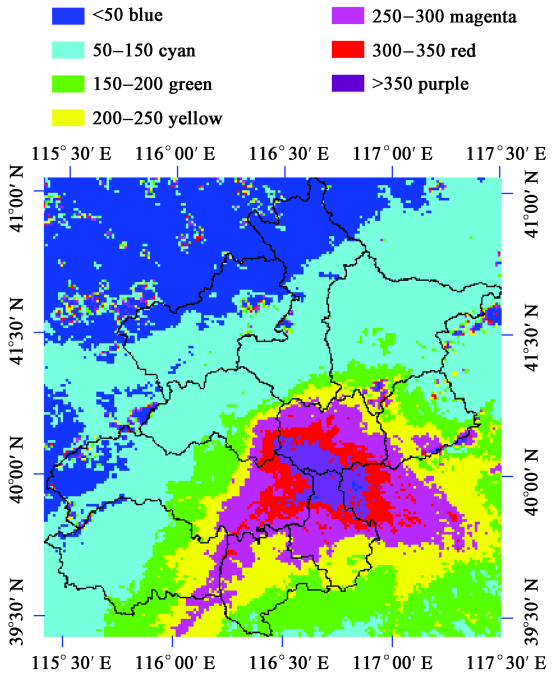

Fig. 4 Distribution of PM_{10} from MODIS in Beijing (2003/8/4; μg/m^3).

Table 2 Mean temperature (°C) in different districts for the January of 2000 and 2004, Beijing

	Haidian	Chaoyang	Fengtai	Miyun	Tongzhou	Mentougou	Fangshan	Shijingshan
2000	–5.7	–6.5	–5.9	–8.7	–6.1	–6.2	–7.3	–6.3
2004	–2.3	–3.0	–2.7	–5.1	–1.7	–2.5	–3.0	–2.4

was 301 μg/m^3. Observation data of PM_{10} concentration indicated that the lowest values were found for the region along Dingling, Huairou, Yanqing and Miyun reservoir and also the Yufa. Zone was also formed with higher pollutants content lying along Tongzhou and Fengtai. This result was in good agreement with the information extracted from MODIS data.

The development of Beijing City was circle-shaped from Forbidden City to outskirt, which led to decreasing pollution from downtown to outskirt. Because of weak south wind, the pollution center was moved to northeast direction from center, forming a new one at the convergence point between Tongzhou and Shunyi. In the zone connecting Beijing downtown and Fangshan there are many heavy chemical industries and construction industries, which produced many pollutants. More than 500 m-high Xishan Mountain prevented the dissipation of pollutants and formed the convergence zone of pollutants before the mountain. The pollutant convergence zone from Tongzhou to Hebei province occurred with a rather low probability because pollutant resources are fewer.

3 Discussion

ACR, as the medial product of the dense dark vegetation method, is proved in this study to be better than the aerosol optical thickness for monitoring particles, for the reason of no look-up table needed, which can introduce an error.

As for dry-clean air, the concentration of aerosol is low. And furthermore stronger wind and precipitation will decrease further the concentration of aerosol, leading to little difference of aerosol concentration. The extraction of information of aerosol will be influenced by surface reflectance. Ambient humidity changes could also affect the response of the instrument of TEOM strongly, which can bring about some errors.

Therefore the aerosol data extracted from MODIS are not good when air pollution is very low. Table 1 indicates that if the concentration of PM_{10} is lower than 80 μg/m^3, there is no significant correlation between PM_{10} and ACR. When air pollution becomes heavier, especially when the concentration of PM_{10} is higher than 100 μg/m^3, because of regional atmospheric stabilization, pollutants accumulate gradually, and the pollution centers come into being and become clear.

Errors will be sure to occur when information is abstracted from MODIS data. Firstly, the extinction from air molecules will be different from location to location. We assume this disturbance as a constant value, which will lead to certain error. Secondly, the surface reflectance of the visible light band is assumed based on the apparent reflectance of 2.1 μm infrared band, and the statistic relation is also highly dependent on ground condition. Lower surface reflectance will be better, otherwise larger error will occur. However, seldom large homogenous ground can be found in Beijing and surface reflectance will be different for different places, which appears some error effects. Furthermore, the monitoring stations for PM_{10} are located mainly in downtown and less in outskirts, which to some degree influenced the results. Influences from clouds are also not effectively avoided. In addition, different kinds of clouds will exert different degrees of influences on information extraction.

4 Conclusions

Some interesting results were obtained based on above research.

(1) Two zones featured by heavy pollution were found, one is in Beijing downtown, the other is the pollution zone lying before Xishan Mountain south-west to downtown. The location and area of these two pollution zones are variable, which sometimes converge together when heavier pollution events occur.

(2) With the development of city center and towns, Beijing is extending with enlarging air pollution. At the same time, the expansion of pollution zone along main transport lines is obvious. The airport Expressway, Badaling Expressway and Jing-Shi Expressway etc., are now pollution stretch zones.

(3) The two pollution zones are also the center of the Beijing heat island. There may exist a cause-effect relationship between heat island effect and the existence of pollutant zones, which needs further research.

References

Ackerman S A, Strabala K I, Menzel W P *et al*., 1998. Discriminating clear-sky from clouds with MODIS[J]. J Geophys Res, 103(D24): 32141–32157.

Beeson W L, Abbey D E, Knutsen S F, 1998. Long-term concentrations of ambient air pollutants and incident lung cancer in California Adults: Results from the AHSMOG Study[J]. Environ Health Perspect, 106: 813–822.

Berico M, Luciani A, Formignani M, 1997. Atmospheric aerosol in an urban area–measurement of TSP and PM_{10} standards a pulmonary deposition assessment[J]. Atmos Environ, 31(21): 36–59.

Charlson R J, Schwartz S E, Hales J M *et al*., 1992. Climate forcing by anthropogenic aerosols[J]. Science, 255: 423–430.

Chu D A, Kaufman Y J, Ichoku C *et al*., 2002. Validation of MODIS aerosol optical depth retrieval overland[J]. Geophys Res Lett, 29(12): 8007–8010.

Chu D A, Kaufman Y J, Aibordi G *et al*., 2003. Global monitoring of air pollution over land from the Earth Observing System–Terra Modierate Resolution Imaging Spectroradiometer (MODIS)[J]. J Geophs Res, 108(D21): 4661–4677.

Griggs M, 1975. Measurement of atmospheric aerosol optical thickness over water using ERTS-1 data[J]. J Air Pollut Contr Assoc, 25: 622–626.

Hutchison K D, 2003. Applications of MODIS satellite data and products for monitoring air quality in the state of Texas[J]. Atmospheric Environmnet, 37: 2403–2412.

IPCC (Intergovernmental Panel on Climate Change), 2001. Climate change 2001: the scientific basis[M]. Cambridge, U. K.: Cambrige University Press.

Kaufman Y J, Sendra C, 1988. Algorithm for automatic atmospheric corrections to visible and near-IR satellite imagery[J]. Int J Remote Sens, 87: 5221–5227.

Kaufman Y J, Tanre D, Remer L *et al*., 1997. Remote sensing of tropospheric aerosols from EOS MODIS overland[J]. J Geophs Res, 102: 17051–17067.

Kaufman Y J, Tanre D, Dubovik O *et al*., 2001. Absorption of sunlight by dust as inferred from satellite and ground-based remote sensing[J]. Geophys Res L&T, 28(8): 1479–1482.

Li X J, Liu Y J, Qiu H *et al*., 2003: Retrieval method for optical thickness of aerosol over Beijing and its vicinity by using the MODIS data[J]. ACTA Meteorologica Sinica, 61(5): 580–592.

Mao J T, Li C C, Zhang J H *et al*., 2002. The comparison of remote sensing aerosol optical depth from MODIS data and ground sun-photometer observations[J]. Journal of Applied Meteorological Science, 13: 127–135.

Mekler Y H, Quenzel G O, Marcus I, 1977. Relative atmospheric aerosol concentration from ERTS observations[J]. J Geophs Res, 82: 967–970.

Taylor K E, and Penner J E, 1994. Response of the climate system to atmospheric aerosols and greenhouse gases[J]. Nature, 369: 734–737.

USEPA (US Environmental Protection Agency), 1990. Title I – Provisions for attainment and maintenance of national ambient air quality standards-zone, carbon monoxide and PM_{10} nonattainment provisions[Z]. In: Clean air act amendments of 1990, Detailed Summary of Titles. 24–28.

Wang J, Christopher S A, 2003. Intercomparison between satellite-derived aerosol optical thickness and $PM_{2.5}$ mass: Implications for air quality studies[J]. Geophys Res Lett, 30(21): 2095–2098.

Yu J H, Yu T, Wei Q *et al*., 2004. Characteristics of mass concentration variations of PM_{10} and $PM_{2.5}$ in Beijing area[J]. Research of Environmental Sciences, 17(1): 45–47.

Zhang G Z, Xu X D, Yang J Z *et al*., 2002. A study of characteristics and evolution of urban heat island over Beijing and its surrounding area[J]. Journal of Applied Meteorological Science, 13: 43–50.